

Study of granular drag force for intruder moving with non-uniform velocities using Discrete Element Method



Author

HUSNAIN MURTAZA

Regn Number

00000205135

Supervisor

DR. SYED ALI ABBAS ZAIDI

DEPARTMENT OF MECHANICAL ENGINEERING  
SCHOOL OF MECHANICAL & MANUFACTURING ENGINEERING  
NATIONAL UNIVERSITY OF SCIENCES AND TECHNOLOGY  
ISLAMABAD  
JANUARY, 2020

Study of granular drag force for intruder moving with non-uniform  
velocities using Discrete Element Method

Author

HUSNAIN MURTAZA

Regn Number


00000205135

A thesis submitted in partial fulfillment of the requirements for the degree of  
MS Mechanical Engineering

Thesis Supervisor:

DR. SYED ALI ABBAS ZAIDI


Thesis Supervisor's Signature: \_\_\_\_\_



DEPARTMENT OF MECHANICAL ENGINEERING  
SCHOOL OF MECHANICAL & MANUFACTURING ENGINEERING  
NATIONAL UNIVERSITY OF SCIENCES AND TECHNOLOGY  
ISLAMABAD  
JANUARY, 2020

## THESIS ACCEPTANCE CERTIFICATE

Certified that final copy of MS thesis written by Mr. Husnain Murtaza Registration No. 00000205135 of SMME has been vetted by undersigned, found complete in all aspects as per NUST Statutes/Regulations, is free of plagiarism, errors, and mistakes and is accepted as partial fulfillment for award of MS/MPhil degree. It is further certified that necessary amendments as pointed out by GEC members of the scholar have also been incorporated in the said thesis.

Signature with stamp:  Dr. Ali Abbas Zaidi  
Assistant Professor  
School of Mechanical &  
Manufacturing Engineering  
(SMME) NUST, Islamabad

Name of Supervisor: Dr. Syed Ali Abbas Zaidi

Date: \_\_\_\_\_

Signature of HoD with stamp: \_\_\_\_\_

Date: \_\_\_\_\_

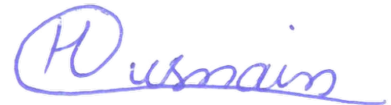
### Countersign by

Signature (Dean/Principal): \_\_\_\_\_

Date: \_\_\_\_\_

## **Declaration**

I certify that this research work titled “*Study of granular drag force for intruder moving with non-uniform velocities using Discrete Element Method*” is my own work. The work has not been presented elsewhere for assessment. The material that has been used from other sources it has been properly acknowledged / referred.



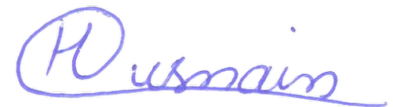
Signature of Student

**HUSNAIN MURTAZA**

**2019-NUST-MS-Mech-00000205135**

## **Language Correctness Certificate**

This thesis has been read by an English expert and is free of typing, syntax, semantic, grammatical and spelling mistakes. Thesis is also according to the format given by the university.



Signature of Student

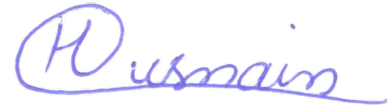
**HUSNAIN MURTAZA**

**2019-NUST-MS-Mech-00000205135**

Signature of Supervisor

## **Plagiarism Certificate (Turnitin Report)**

This thesis has been checked for Plagiarism. Turnitin report endorsed by Supervisor is attached.



Signature of Student

**HUSNAIN MURTAZA**

**2019-NUST-MS-Mech-00000205135**

Signature of Supervisor

## **Copyright Statement**

- Copyright in text of this thesis rests with the student author. Copies (by any process) either in full, or of extracts, may be made only in accordance with instructions given by the author and lodged in the Library of NUST School of Mechanical & Manufacturing Engineering (SMME). Details may be obtained by the Librarian. This page must form part of any such copies made. Further copies (by any process) may not be made without the permission (in writing) of the author.
- The ownership of any intellectual property rights which may be described in this thesis is vested in NUST School of Mechanical & Manufacturing Engineering, subject to any prior agreement to the contrary, and may not be made available for use by third parties without the written permission of the SMME, which will prescribe the terms and conditions of any such agreement.
- Further information on the conditions under which disclosures and exploitation may take place is available from the Library of NUST School of Mechanical & Manufacturing Engineering, Islamabad.

## **Acknowledgements**

I am thankful to my Creator Allah Subhana-Watala to have guided me throughout this work at every step and for every new thought which You setup in my mind to improve it. Indeed, I could have done nothing without Your priceless help and guidance. Whosoever helped me throughout the course of my thesis, whether my parents or any other individual was Your will, so indeed none be worthy of praise but You.

I am profusely thankful to my beloved parents who raised me when I was not capable of walking and continued to support me throughout in every department of my life.

I would also like to express special thanks to my supervisor Dr. Syed Ali Abbas Zaidi for his help throughout my thesis. Each time I got stuck in something, he came up with the solution. Without his help I wouldn't have been able to complete my thesis. I appreciate his patience and in-depth guidance throughout the whole thesis.

I would also like to thank Dr Emad Uddin, Dr Zaib Ali and Dr Waqas Hassan Tanveer for being on my thesis guidance and evaluation committee.

Finally, I would like to express my gratitude to all the individuals who have rendered valuable assistance to my study.



*Dedicated to my exceptional parents and teachers whose tremendous support and cooperation led me to this wonderful accomplishment.*

## Abstract

Like in fluids, objects moving in granular materials experience drag force. In granular materials this drag force on the object, or “intruder,” arises from inter-particle friction, as well as the cyclic creation and buckling of force chains within the material. The aim of this work is to investigate whether and how the acceleration of object affects this drag force. This is done by simulating the behavior of granular materials using discrete element method (DEM). Study includes a series of drag tests which involve pulling an intruder through stationary granular packing with a prescribed acceleration profile. The system is parametrized using the dimensionless Froude number  $Fr = 2v/\sqrt{gR}$ , where  $v$  is the instantaneous speed of intruder of radius  $R$ . Simulation results evidence the presence of a rate-dependent regime ( $Fr < 1$ ) where intruder’s acceleration strongly influences the drag force. This behavior is fundamentally different from steady state motion where this regime is governed by friction coefficient of the system and immersion depth of intruder. This behavior is also found in contrast with fluids where an accelerating body in fluid medium experiences an increase in drag due to added mass effect. This peculiar behavior of granular material is determined to be due to the formation of highly anisotropic force chains and their complex dynamics as they evolve under load.

**Keywords:** Granular materials, Granular flows, Granular drag, Virtual mass, Discrete element method

# Table of Contents

<b>Declaration .....</b>	<b>i</b>
<b>Language Correctness Certificate.....</b>	<b>ii</b>
<b>Plagiarism Certificate (Turnitin Report).....</b>	<b>iii</b>
<b>Copyright Statement .....</b>	<b>iv</b>
<b>Acknowledgements .....</b>	<b>v</b>
<b>Abstract .....</b>	<b>vii</b>
<b>List of Figures .....</b>	<b>ix</b>
<b>List of Tables.....</b>	<b>x</b>
<b>Nomenclature .....</b>	<b>xi</b>
<b>List of Abbreviation.....</b>	<b>xii</b>
<b>CHAPTER 1: INTRODUCTION.....</b>	<b>1</b>
1.1    Background, Scope and Motivation .....	1
<b>CHAPTER 2: LITERATURE REVIEW .....</b>	<b>3</b>
<b>CHAPTER 3: ANALYTICAL MODELS AND NUMERICAL METHODOLOGY .....</b>	<b>5</b>
3.1    Discrete Element Method.....	5
3.2    Simulation Setup .....	9
3.3    Benchmarks:.....	14
3.3.1    Steady drag on horizontally moving intruder .....	14
3.3.2    Steady drag on vertically moving intruder .....	15
<b>CHAPTER 4: RESULTS AND DISCUSSION .....</b>	<b>17</b>
4.1    Parametric Study:.....	18
4.1.1    Effect of particle density on virtual mass force .....	18
4.1.2    Effect of particle stiffness on virtual mass force .....	20
4.1.3    Effect of particle coefficient of restitution on virtual mass force .....	21
4.1.4    Effect of particle friction coefficient on virtual mass force .....	22
<b>CHAPTER 5: CONCLUSION .....</b>	<b>25</b>
<b>CHAPTER 6: FUTURE RECOMMENDATIONS .....</b>	<b>26</b>
<b>REFERENCES .....</b>	<b>27</b>

## List of Figures

<b>Figure 3-1:</b> Schematic diagram of soft-sphere model .....	5
<b>Figure 3-2:</b> Schematic diagram of linear-spring–dashpot model (LSD) contact model.....	6
<b>Figure 3-3:</b> Two particles making contact .....	7
<b>Figure 3-4:</b> Particle $i$ in contact with surrounding particles.....	8
<b>Figure 3-5:</b> Discrete Element Method flowchart. ....	9
<b>Figure 3-6:</b> Simulation Setup.....	10
<b>Figure 3-7:</b> Section Plane $x - x'$ .....	11
<b>Figure 3-8:</b> Simulation domain sliced along $x - x'$ plane .....	11
<b>Figure 3-9:</b> Contour plot of velocity magnitude of particles in simulation. The inset shows the zone of influence for intruder velocity of 0.1m/s.....	12
<b>Figure 3-10:</b> Intruder velocity profile .....	13
<b>Figure 3-11:</b> Comparison of granular drag force on a spherical intruder in a granular bed at low Froude number Hilton, J. E., & Tordesillas, A. (2013).....	15
<b>Figure 3-12:</b> Simulation setup for vertical intrusion .....	16
<b>Figure 3-13:</b> Granular drag force $F$ on intruder with different intruder velocities.....	16
<b>Figure 4-1</b> Non-dimensional drag force plotted against Froude number for different accelerations .....	18
<b>Figure 4-2:</b> Non-dimensional drag force plotted against Froude number different accelerations (a) Particle Density 2500 kg/m <sup>3</sup> (b) Particle Density 5000 kg/m <sup>3</sup> .....	19
<b>Figure 4-3:</b> Non-dimensional drag force plotted against Froude number for different accelerations (a) Particles stiffness 800N/m (b) Particles stiffness 8000N/m .....	20
<b>Figure 4-4:</b> Non-dimensional drag force plotted against Froude number for different accelerations (a) Coefficient of restitution 0.7 (c) Coefficient of restitution 0.2 .....	21
<b>Figure 4-5:</b> Non-dimensional drag force plotted against Froude number for different accelerations (a) Coefficient of Friction 0.1 (b) Coefficient of Friction 0.5 .....	22
<b>Figure 4-6</b> Particles accelerated with intruder ( $NXVel = Vintruder/Vparticles$ ) for Froude 0.01 (a) acceleration 0 m/s <sup>2</sup> (b) acceleration 0.1 m/s <sup>2</sup> (d) acceleration 10 m/s <sup>2</sup> .....	23
<b>Figure 4-7</b> Non-dimensional drag force plotted against Froude number for different accelerations. Discrete points represent simulation results and dotted line represent Eqn. 4.2 with appropriate fitting parameters.....	24

## List of Tables

<b>Table 4-1:</b> Simulation parameters used.....	13
<b>Table 4-2:</b> Particle Material Properties .....	14
<b>Table 4-3:</b> Intruder Material Properties.....	14
<b>Table 5-1:</b> Fit coefficients .....	24

## Nomenclature

$Fr$	Froude Number
$v$	Velocity of intruder
$R$	Radius of intruder
$g$	Gravitational acceleration
$k$	Spring stiffness
$\eta$	Damping coefficient
$f$	Friction coefficient
$F$	Contact force
$G$	Relative velocity vector
$n$	Normal unit vector
$t$	Tangential unit vector
$r$	Radius of particle
$d_p$	Diameter of particle
$D$	Diameter of intruder
$\rho$	Density
$F^*$	Average non-dimensional force on intruder, non-Dimensionalized by particle weight
$F'$	Unsteady drag non-dimensionalized by steady drag.
$\phi$	Packing fraction
subscripts	
$n$	Normal component
$t$	Tangential component
$x$	x-direction
$z$	z-direction

## List of Abbreviation

DEM	Discrete Element Method
LSD	Linear-spring-dashpot model

## CHAPTER 1: INTRODUCTION

Granular materials are developed by conglomeration of discrete macroscopic particles and are ubiquitous both in nature and industrial applications. Granular materials, like fluids, yield under shear stress constituting granular flows. Such flows are encountered in food, pharmaceutical, chemical, metallurgical, agricultural, mining and construction industries (Antony, Hoyle, & Ding, 2004) as well as in natural processes such as landslides (Darve & Laouafa, 2000), dune migration, erosion/deposition processes and coastal geomorphology (Bishop, Momiji, Carretero-González, & Warren, 2002).

### 1.1 Background, Scope and Motivation

In literature, various studies have shown interesting similarities between flowing granular materials and viscous fluids. Some of them include: Magnus Effect (Kumar, Dhiman, & Reddy, 2019), Kelvin-Helmholtz instability (Goldfarb, Glasser, & Shinbrot, 2002), Rayleigh-Plateau (Prado, Amarouchene, & Kellay, 2011), Rayleigh-Taylor instability (Vinningland, Johnsen, Flekkøy, Toussaint, & Måløy, 2007), capillary action (Fan, Parteli, & Pöschel, 2017) etc. Despite these similarities, there are also some anomalies such as jamming (Reddy, Kumar, Reddy, & Talbot, 2018), Reynolds' dilation (Reynolds, 1885) etc., which are unique to granular media. These characteristics place granular materials in a unique position between fluids and solids (Jaeger, Nagel, & Behringer, 1996). This behavior of granular materials is attributed to two unique properties of granular materials i.e. ordinary temperature plays no role, and the interactions between grains are dissipative because of static friction and the inelasticity of collisions (Jaeger et al., 1996).

A body immersed in granular medium, like fluids, experiences resistance force called granular drag force ( $F_d$ ) while moving through the medium. Granular drag force is a fundamental property of granular materials. The granular drag force in granular materials arise from the complex nature of stress propagation in the bulk of the medium where the drag is caused not only by the grains immediately in front of the object but also the grains in the successive layers supporting them (R. Albert, Pfeifer, Barabási, & Schiffer, 1999).

Understanding granular drag force is important for applications where objects (intruders) are moving through granular media such as agitation blades in granular mixers, agricultural tillage



equipment and drilling (Okorie, 2017; Rhodes, 1990; Tijskens, Ramon, & De Baerdemaeker, 2003). A better understanding granular drag force can lead to optimization of many industrial processes and better understanding of natural phenomenon. This study aims to perform DEM simulations to study the unsteady drag experienced by intruder and detect and evaluate the fluid equivalent virtual mass force in granular systems.

## CHAPTER 2: LITERATURE REVIEW

In literature, there is general consensus that for simple case of rigid intruder penetrating granular media, granular drag force can be modeled by Eqn. 2.1 (Katsuragi & Durian, 2007; Takada & Hayakawa, 2017; Tsimring & Volfson, 2005; Umbanhowar & Goldman, 2010):

$$F_d(z, v) = F_o + F(z) + F(v) \quad (2.1)$$

Where  $z$  is the depth of penetration of intruder in granular bed and  $v$  is the velocity of the intruder relative to granular bed.  $F_o$  is the frictional drag force,  $F(z)$  is the depth dependent drag force and  $F(v)$  is the velocity dependent drag force.  $F_o$  and  $F(z)$  constitute hydrostatic-like component of the granular drag force while  $F(v)$  represent the hydrodynamic-like component of granular drag force.

Drag force on intruders moving in horizontal direction (perpendicular to gravity) can be parametrized by using dimensionless Froude number. Froude number is defined as the ratio of two characteristic time scales of an intruder moving horizontally in granular bed. First time scale ( $t_p = 2\sqrt{R/g}$ ) is the time for particle to fall back in granular bed after the intruder moves past it and the second time scale ( $t_i = R/v$ ) is the time characterizing intruder's forward motion. The ratio between the two time scales is given as  $Fr = t_p/t_i = 2v/\sqrt{gR}$ , where  $v$  and  $R$  are intruder velocity and radius respectively and  $g$  is the gravitational acceleration.

For small intruder velocities ( $Fr < 1$ ), contribution of hydrodynamic component is negligible and thus the drag force can be represented with only rate independent hydrostatic component (Soller & Koehler, 2006). At high intruder velocities ( $Fr > 1$ ) the hydrodynamic component dominates (Hilton & Tordesillas, 2013; Kumar, Reddy, Takada, & Hayakawa, 2017).

Eqn. 2.1, however, does not incorporate unsteady effects due to relative change of velocity (acceleration or deceleration) of intruder. In fluids, it is well known that unsteady drag force acting on a body is greater than steady drag force due to presence of "virtual mass force". Virtual mass force consists of two components: Basset force and added mass effect. Basset force is due to temporal delay in boundary layer formation when the relative velocity of submerged body changes. Added mass effect is the additional work done by the body to accelerate or decelerate the surrounding fluid. (Brennen, 1982). Since added mass is caused due to the inertia of the fluid being accelerated, it depends on density of fluid and independent of the viscosity of fluid.. Situations in which the density of the fluid is comparable or greater than the density of accelerating body, added mass can be significant and neglecting it can introduce significant errors into a calculation. Due to its significance added mass is well studied phenomenon in fluid mechanics and governing equations are well developed.

Despite its significance, virtual mass force for granular flows has not been extensively studied. It has been shown in literature (Aguilar & Goldman, 2016; Katsuragi & Durian, 2014; Lohse, Rauhe, Bergmann, & Van Der Meer, 2004) that for intruders penetrating granular media with non-uniform velocities experience an increase in inertia and neglecting this can result in erroneous predictions. Considering the effect of virtual mass force Eqn. 2.1 takes the form given in Eqn. 2.2 (Aguilar & Goldman, 2016; Athani & Rognon, 2019)

$$F_d(z, v) = F_o + F(z) + F(v) + F(a) \quad (2.2)$$

Where  $F(a)$  is the component of drag force due to the relative acceleration of the intruder.

All the studies discussed so far only consider vertical penetrations. To Author's knowledge no studies has been done to investigate virtual mass force acting on horizontally moving intruder. Differentiation between vertical and horizontal system is important in granular systems because in contrast with horizontal systems gravity and flow direction in vertical systems are parallel and there is no comparable time scale as  $t_p$ , and thus, there is no transition at  $Fr = 1$ . This study aims to address the presence of virtual mass force in horizontally driven system, effects of different particle material properties on the virtual mass force and later develop relation for virtual mass force in granular media

# CHAPTER 3: ANALYTICAL MODELS AND NUMERICAL METHODOLOGY

## 3.1 Discrete Element Method

In this Study, Discrete element method (DEM) (Cundall & Strack, 1979) is used to simulate granular material. Two main assumptions are made in this model to simplify the mechanics of particle collisions. First, it is assumed that the influence of particle of interest is only limited to its immediate neighbors. This is made feasible by assuming a small time step so that disturbances do not travel far. Second, the deformation of colliding particles is replaced by the overlap of two particles. Due to this assumption is this model is also known as soft sphere model. **Figure 3-1** shows the schematic of soft sphere model.

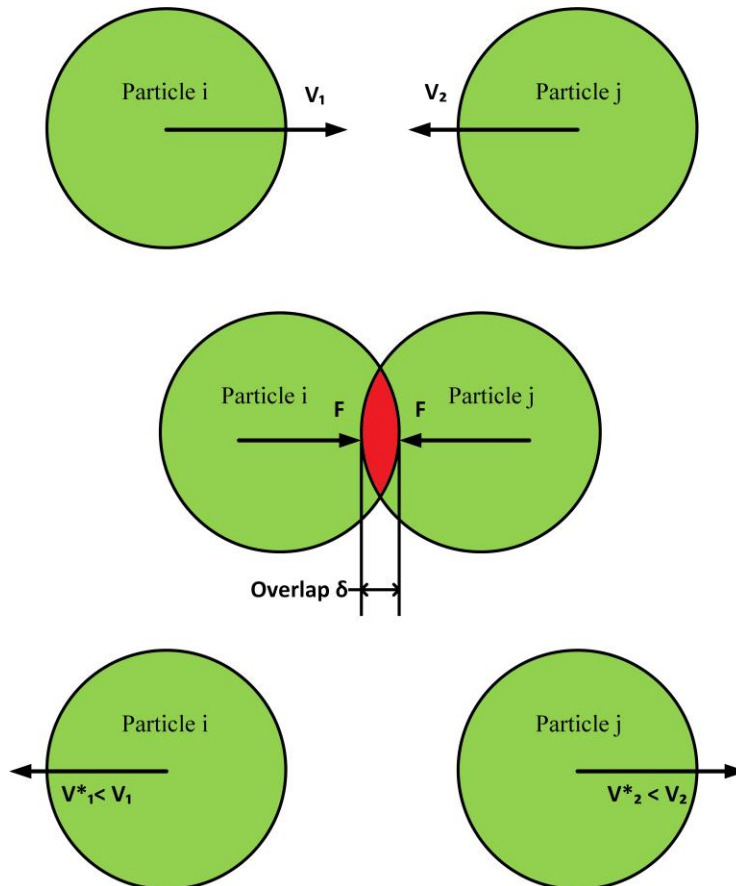


**Figure 3-1:** Schematic diagram of soft-sphere model

Various contact models are used in DEM simulations (Rojek, 2018) to calculate contact forces. This study uses linear-spring–dashpot model (LSD) to calculate contact forces. LSD allows for smaller stiffness values to be selected, which allows a larger time step to be used (Malone & Xu, 2008). This enables LSD to be less computationally expensive than other more complex models available in literature. LSD has also been found to be reasonably accurate in predicting the behavior of granular flow dynamics. (Ji & Shen, 2006; Mishra & Murty, 2001). LSD uses linear spring (with stiffness  $k$ ) along with a dashpot (with damping coefficient  $c$ ) to simulate inter-particle and particle-wall interactions. A friction slider is also introduced to model the relative sliding of particles. A schematic diagram of the model is shown in **Figure 3-2**.

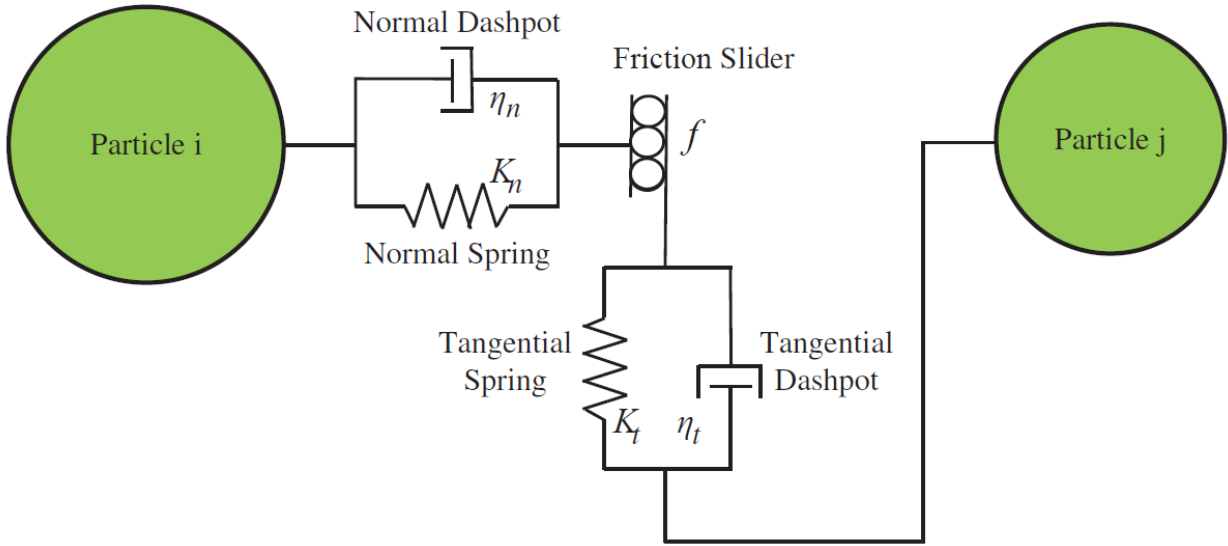


**Figure 3-2:** Schematic diagram of linear-spring–dashpot model (LSD) contact model

Particle-particle and particle-wall contact force,  $\mathbf{F}_c$ , is the sum of normal,  $\mathbf{F}_n$ , and tangential,  $\mathbf{F}_t$ , components.  $\mathbf{F}_n$  and  $\mathbf{F}_t$  calculated from normal and tangential overlap when the particles overlap during collision. Schematic showing two particle making contact is shown in **Figure 3-3**. Using LSD  $\mathbf{F}_c$  can be calculated using Eqn. 3.1-3.3.

$$\mathbf{F}_c = \mathbf{F}_n + \mathbf{F}_t \quad (3.1)$$

$$\mathbf{F}_n = (-K_n \delta_n - \eta_n \mathbf{G} \cdot \mathbf{n}) \mathbf{n} \quad (3.2)$$

$$\mathbf{F}_t = -\min(f |\mathbf{F}_n| \mathbf{t}, K_t \delta_t + \eta_t \mathbf{G}_t) \quad (3.3)$$

Here,  $K$  and  $\eta$  represent spring stiffness and damping coefficient respectively. Subscript  $t$  and  $n$  represent normal and tangential directions of particle-particle contact along unit vectors  $\mathbf{t}$

and  $\mathbf{n}$  respectively.  $\mathbf{G}$  is the relative velocity of colliding particles,  $G_t$  is the slip velocity of the contact point and  $f$  is the particle coefficient of friction.

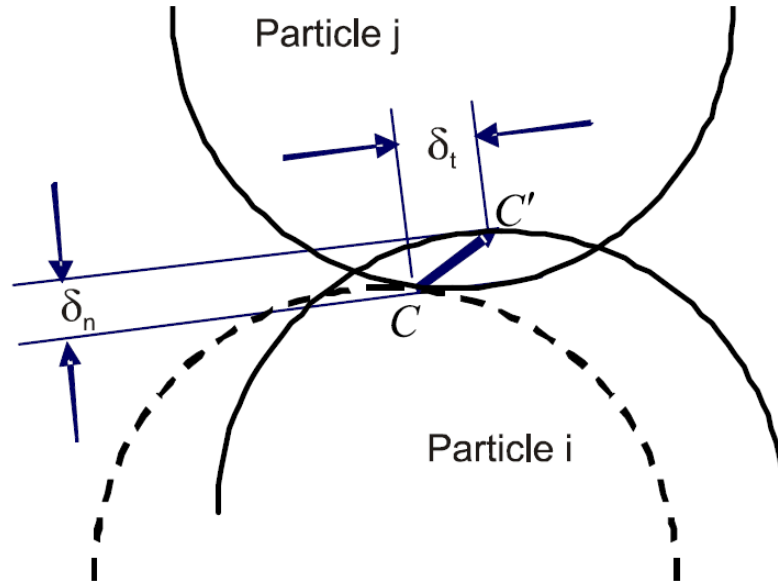


**Figure 3-3:** Two particles making contact

At any instant particle can be in contact with more than one particle as shown in the **Figure 3-4**. In that case the total contact force and torque on the particle  $i$  can be given as the summation of the individual particle forces as given in Eqn. 3.4,3.5.

$$\mathbf{F}_i = \sum_j (\mathbf{F}_{nij} + \mathbf{F}_{tij}) \quad (3.4)$$

$$\mathbf{T}_i = \sum_j (r\mathbf{n} \times \mathbf{F}_{tij}) \quad (3.5)$$

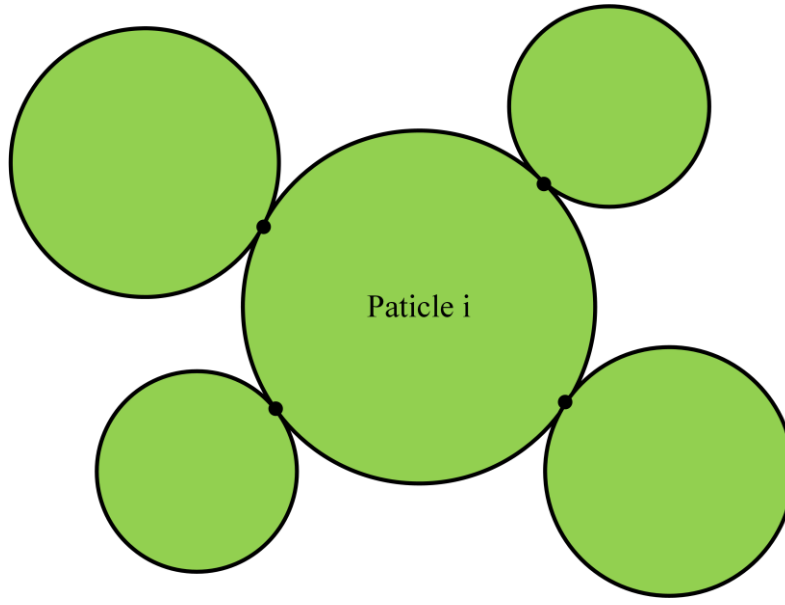


**Figure 3-4:** Particle  $i$  in contact with surrounding particles

Particle acceleration is calculated from contact force ( $F_c$ ) using Newton's second law. Particle velocity and position can then be calculated by integrating acceleration. In this study, for higher accuracy, the author has decided to use the Fourth-order Adams-Bashforth time integration scheme for integration.

A general summary of the DEM algorithm is shown in Figure 3-5.

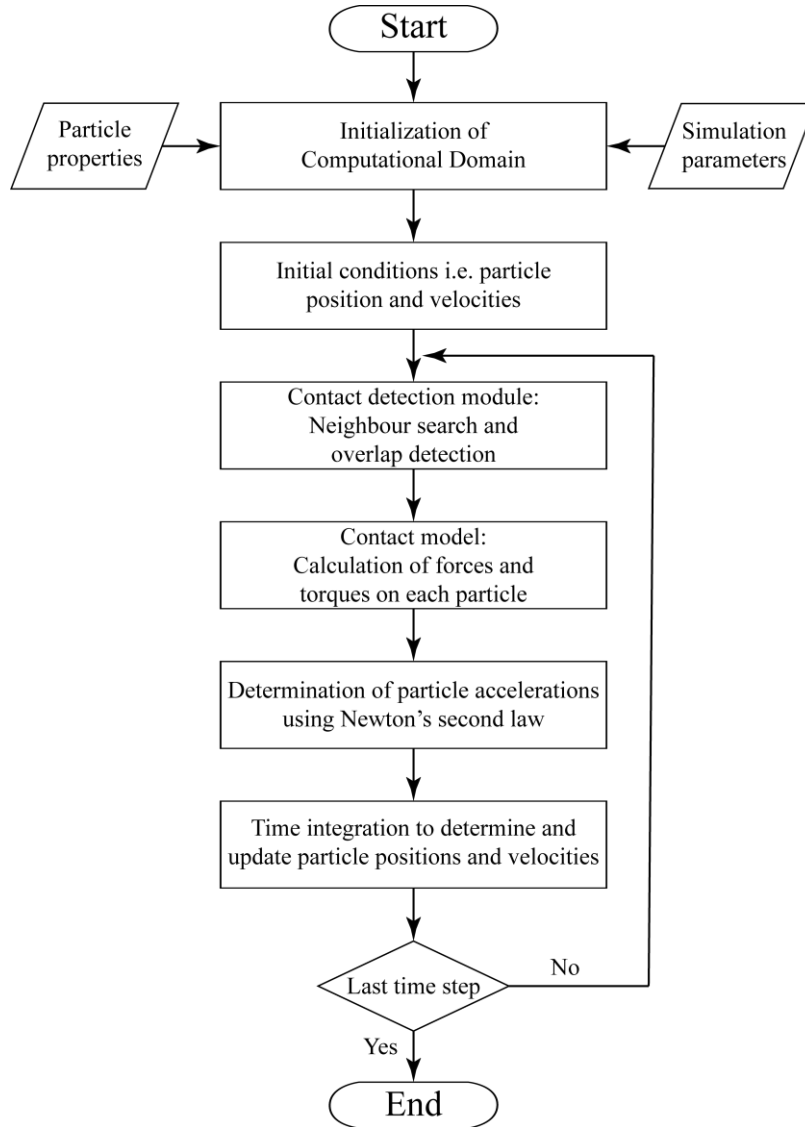


**Figure 3-5:** Discrete Element Method flowchart.

### 3.2 Simulation Setup

In simulations, random arrangement of particles is used which is obtained by allowing the particles to fall under action of gravity from initial cubic arrangement with random velocities. Due to dissipative nature of particle collisions, particles come to rest after some time, constituting granular bed. Granular bed of  $160d_p \times 65d_p \times 40d_p$  length, width and height respectively is used to carry out simulations. Where,  $d_p$  is the diameter of particles constituting the bed. Periodic boundary condition is used in  $x$  and  $z$  directions and a wall is defined at the bottom ( $y = 0$ ).



A large spherical particle is used as intruder. Particle-intruder collisions are modeled same as inter-particle collisions using Eqn. 3.1-3.3. Total drag force on intruder is obtained by summing of all the individual particle forces acting on intruder. Initial configuration as shown in **Figure 3-6** is obtained by immersing intruder in the granular bed and allowing the whole arrangement to settle down. To observe the intruder and the behavior of particles around the intruder the domain is often sliced along the plane  $x - x'$  as shown in **Figure 3-7**. Initial configuration sliced along  $x - x'$  and viewed from  $+z$  is shown in **Figure 3-8**.

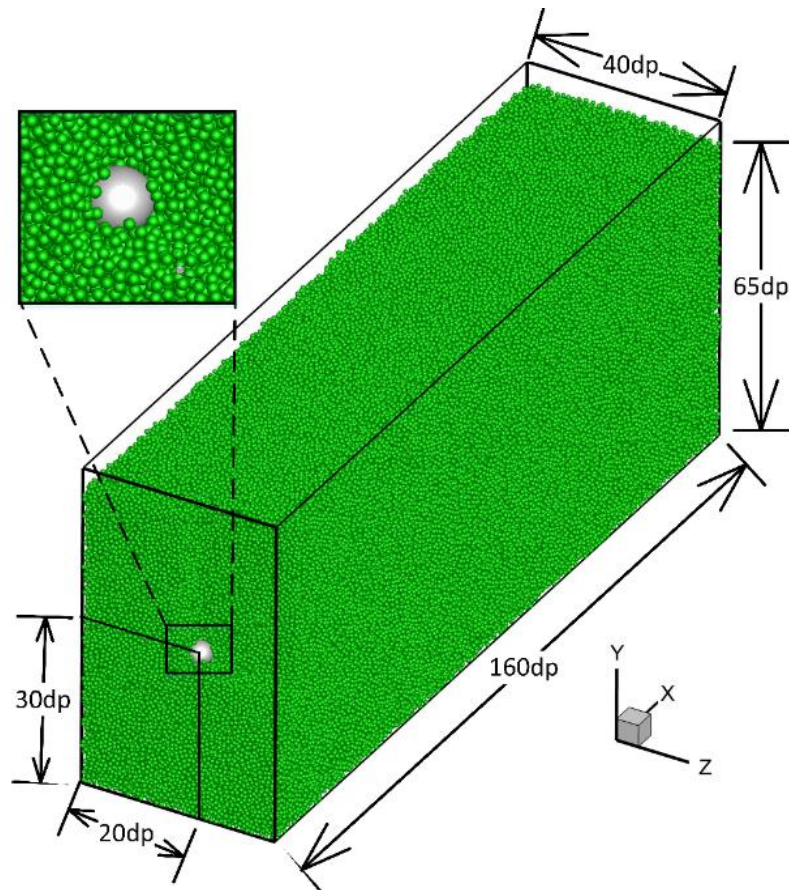


**Figure 3-6: Simulation Setup**

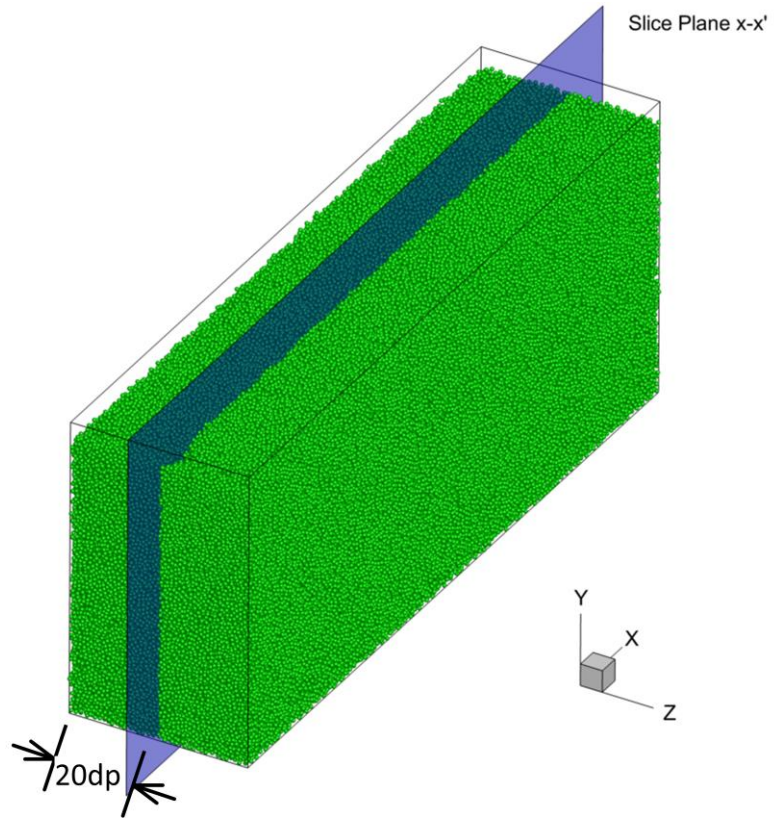


**Figure 3-7:** Section Plane  $x - x'$

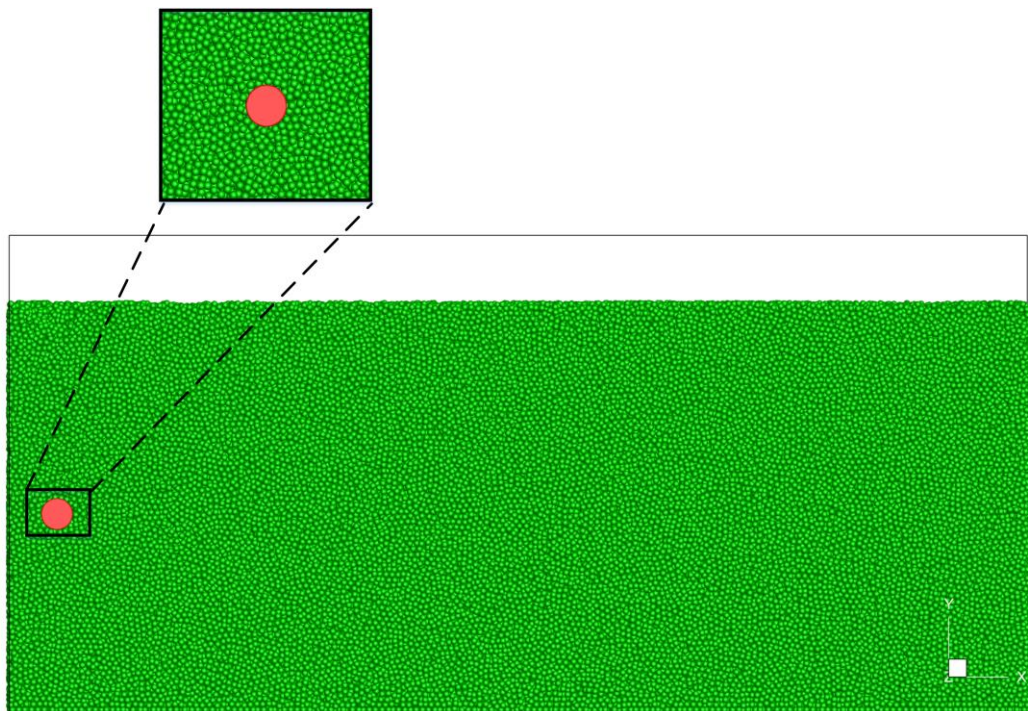


**Figure 3-8:** Simulation domain sliced along  $x - x'$  plane

Spherical intruder of  $5d_p$  is considered for this study. Experiments have shown that to avoid the wall effects the that the ratio of width of domain to intruder diameter should be greater than 5 ( $L/D > 5$ ) (Nelson, Katsuragi, Mayor, & Durian, 2008; Seguin, Bertho, & Gondret, 2008) The domain size chosen is large enough to comply with the aforementioned condition i.e. ( $L/D > 5$ ). To avoid the surface effects, the intruder should be sufficiently below the free surface. This is guaranteed by making sure that the particles at the surface remain undisturbed when the intruder is moving. This can be visually observed by slicing the domain along plane  $x - x'$  as shown in **Figure 3-7** and plotting the absolute particle velocity contour. As seen from **Figure 3-9** the disturbance caused by intruder remains well below the surface.

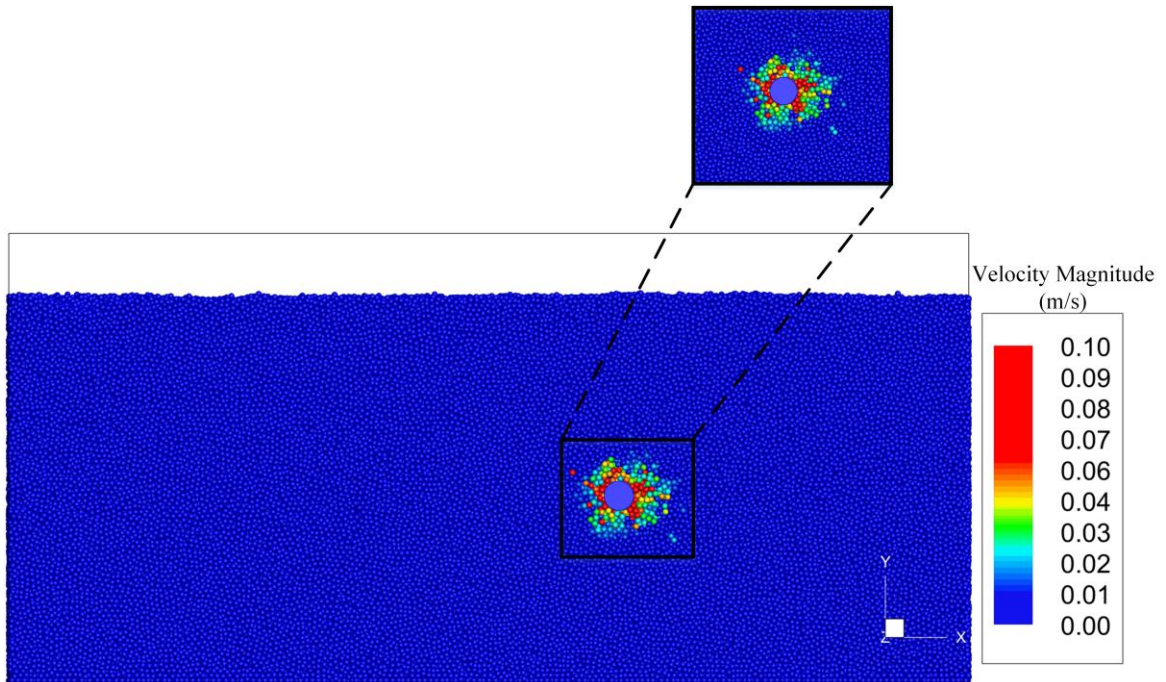


**Figure 3-9:** Contour plot of velocity magnitude of particles in simulation. The inset shows the zone of influence for intruder velocity of 0.1m/s

Time step is of the order of  $10^{-5}s$  which is well below the one-tenth of natural oscillation period of mass spring damper system i.e.  $2\pi\sqrt{m/k}$ . For steady simulations constant velocity along horizontal  $x$  direction is imposed on intruder and constant horizontal acceleration is imposed on the intruder for unsteady simulations. Instantaneous velocity at any time  $t$  for constant acceleration cases is calculated using equation of motion in Eqn. 3.6.

$$v = v_i + at^2 \quad (3.6)$$

Where  $v$  is the instantaneous intruder velocity,  $v_i$  is the initial intruder velocity and  $a$  is the imposed acceleration. Intruder velocity profile is shown in **Figure 3-10**.

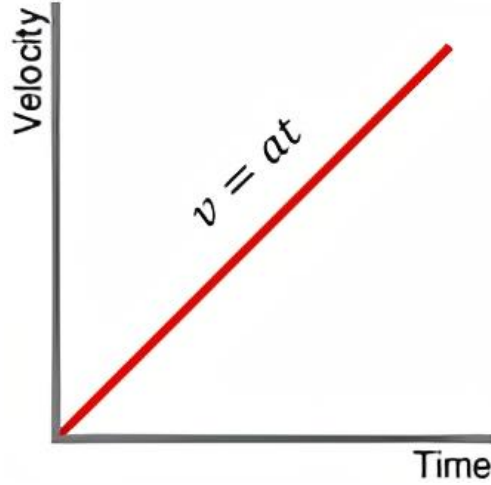


**Figure 3-10:** Intruder velocity profile

For both steady and unsteady simulations a constant gravitational acceleration  $g$  of  $-9.81m/s^2$  is applied in the vertical  $y$  direction. Simulation parameters are summarized in **Table 3-1**

**Table 3-1:** Simulation parameters used.

Parameter	Value
No. of particles	500,000
Diameter of particle ( $d_p$ ) (mm)	1.2
Intruder Diameter ( $D$ ) (mm)	6.0
Gravitational acceleration ( $ms^{-2}$ )	9.81
Domain Size	$160d_p \times 65d_p \times 40d_p$
Time step (s)	$1 \times 10^{-5}$

Particle material parameters are selected to allow for simulation of stiffest possible particles within reasonable amount of time. Particles of density  $2500kg/m^3$ , coefficient of restitution 0.7 friction coefficient 0.1 and elastic modulus  $1MPa$  are defined as baseline and then,

one physical property is varied at one time for the parametric study. Particle properties are summarized in **Table 3-2**. Similarly, intruder material properties are given in **Table 3-3**.

**Table 3-2: Particle Material Properties**

<b>Parameter</b>	<b>Value</b>
Density ( $\rho$ ) ( $kgm^{-3}$ )	2500
Coefficient of friction	0.2
Coefficient of restitution	0.7
Stiffness (normal) ( $Nm^{-1}$ )	800
Stiffness (tangential) ( $Nm^{-1}$ )	700
Poisson's ratio	0.25

**Table 3-3: Intruder Material Properties**

<b>Parameter</b>	<b>Value</b>
Density ( $\rho$ ) ( $kgm^{-3}$ )	2500
Coefficient of friction	0.2
Coefficient of restitution	0.7
Stiffness (normal) ( $Nm^{-1}$ )	800
Stiffness (tangential) ( $Nm^{-1}$ )	700
Poisson's ratio	0.25

### 3.3 Benchmarks:

DEM code is benchmarked for steady state drag by moving the intruder in granular bed, perpendicular to gravity, with constant velocity.

#### 3.3.1 Steady drag on horizontally moving intruder

Figure 3-11 shows the drag experience by intruder (non-dimensionalized by the particle weight) plotted against Froude number. The results show constant drag force for  $Fr < 1$  and linear increase in drag force for  $Fr > 1$ . This behavior is consistent with experimental and simulation data available in literature (R. Albert et al., 1999; Hilton & Tordesillas, 2013; Kumar et al., 2017).

Quantitative comparison with (Hilton & Tordesillas, 2013) shows good correspondence with an maximum error of 7.01%.

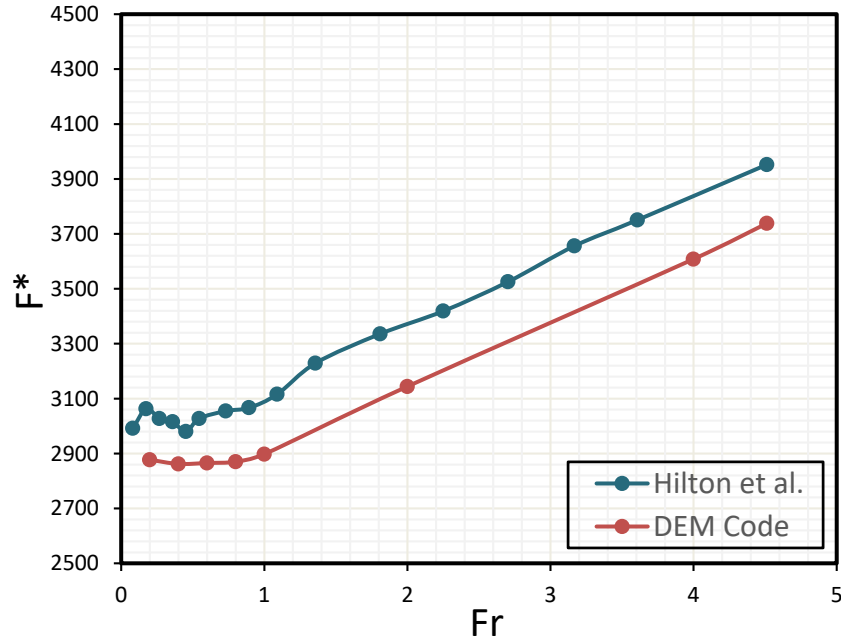


**Figure 3-11:** Comparison of granular drag force on a spherical intruder in a granular bed at low Froude number Hilton, J. E., & Tordesillas, A. (2013).

### 3.3.2 Steady drag on vertically moving intruder

For vertical intrusion benchmark granular bed of dimensions  $80d_p \times 80d_p \times 140d_p$  is used while keeping the particle and intruder material properties same. Simulation setup for vertical intrusion study is shown in Figure 3-12. Figure 3-13 shows the log-log plot of granular drag force plotted against intrusion depth for different intruder intrusion velocities. Intrusion depth is non-dimensionalized by the particle diameter. Drag force ( $F$ ) is plotted when the intruder is fully submerged and before the granular drag force increases drastically due to bottom wall's effect. On the log-log plot the data can be approximated by straight line of slope 1.3. This result is in correspondence with experimental study done by Hill et al where the author proposes power law given in Eqn. 3.7 for vertically penetrating spherical intruder.

$$F = c \left( \frac{z}{d_p} \right)^{1.3} \quad (3.7)$$

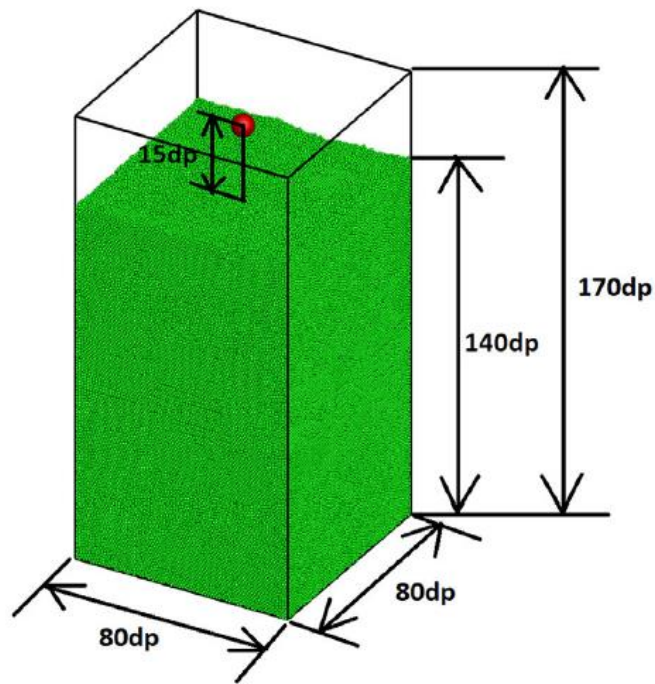


**Figure 3-12:** Simulation setup for vertical intrusion

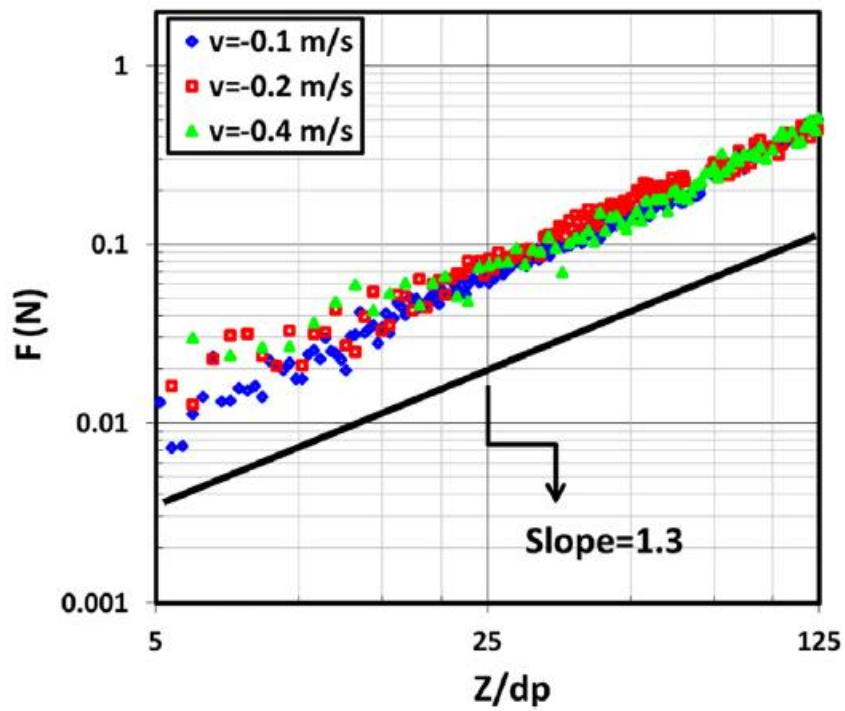


**Figure 3-13:** Granular drag force  $F$  on intruder with different intruder velocities

## CHAPTER 4: RESULTS AND DISCUSSION

Simulation results for intruder moving in granular bed with constant velocity show that drag force can be divided into two regimes parametrized by Froude number. **Figure 3-11** shows non-dimensional drag force ( $F^*$ ) on intruder plotted against Froude number, where  $F^*$  is non-dimensional drag force obtained by dividing the net force on intruder by particle weight. For  $Fr < 1$ , drag force on intruder remains constant. In this regime,  $t_p$  is greater than  $t_i$  and particles have sufficient time to rearrange themselves. Therefore, the resistance to the intruder motion is offered by the local jamming and buckling of force chains (R. Albert et al., 1999; Hilton & Tordesillas, 2013). After Froude number exceeds 1,  $t_p > t_i$  and the grains are fluidized, i.e., grains do not have time to settle into a formation (R. Albert et al., 1999). Drag force is caused by momentum transfer to the intruder due to particles colliding with the intruder (Chehata, Zenit, & Wassgren, 2003). Drag force in this regime increases linearly with velocity (Geng & Behringer, 2005; Hilton & Tordesillas, 2013).

To compare the drag force for accelerating intruder to a non-accelerating intruder the force is non-dimensionalized with steady state drag to obtain non-dimensional drag force  $F'$ . Unsteady drag force acting on accelerating intruder is found to be less than steady drag force acting on non-accelerating intruder for  $Fr < 1$  and equal to steady drag force for  $Fr = 1$ . This reduction in drag is in contrast to fluids where the acceleration of the object in fluid medium causes increase in fluid drag force experienced by the accelerating body due to virtual mass force. Figure 4-1 shows non-dimensional steady and unsteady drag force ( $F'$ ) plotted against Froude number. For steady case where intruder acceleration is zero granular drag force remains constant for  $Fr < 1$ . This is in consensus with the previous discussion on steady drag force. For  $Fr < 1$  granular drag force for non-zero accelerations is always less than zero acceleration case. At  $Fr = 1$ , where transition between gravitational ( $t_p$ ) and inertial ( $t_i$ ) time scale occurs, this drag reduction effect disappears and steady and unsteady drag forces become equal. Unsteady drag force shows an inverse relation with intruder acceleration i.e. increasing the acceleration reduces the drag force. This drag reduction effect is significant for low accelerations while it diminishes at high acceleration. This indicates strong dependence of unsteady drag on the acceleration as well as Froude number.



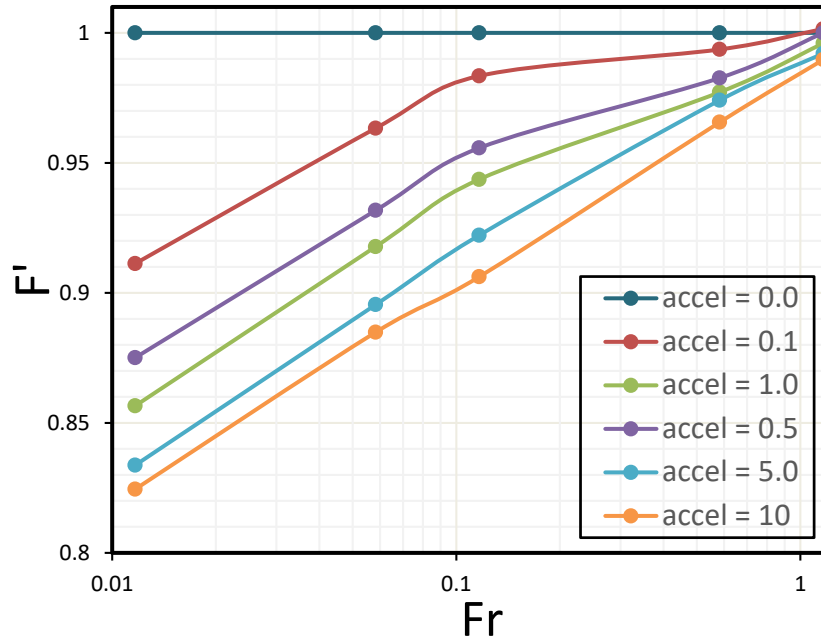


**Figure 4-1** Non-dimensional drag force plotted against Froude number for different accelerations

## 4.1 Parametric Study:

To investigate the effect of material properties on virtual mass force. Material properties of particles and intruder given in **Table 3-2** and **Table 3-3** respectively are considered as baseline and exactly one property is changed for each of the following studies.

### 4.1.1 Effect of particle density on virtual mass force

**Figure 4-2** shows comparison of drag for particles of two different densities i.e.  $2500\text{kg}/\text{m}^3$  and  $5000\text{kg}/\text{m}^3$ . Results indicate a reduction in drag force with increasing density. For example, for Froude number 0.01 A reduction of 0.4% and 0.2% is found for lowest studied acceleration of  $0.1\text{m}/\text{s}^2$  and highest studied acceleration of  $10\text{m}/\text{s}^2$ .

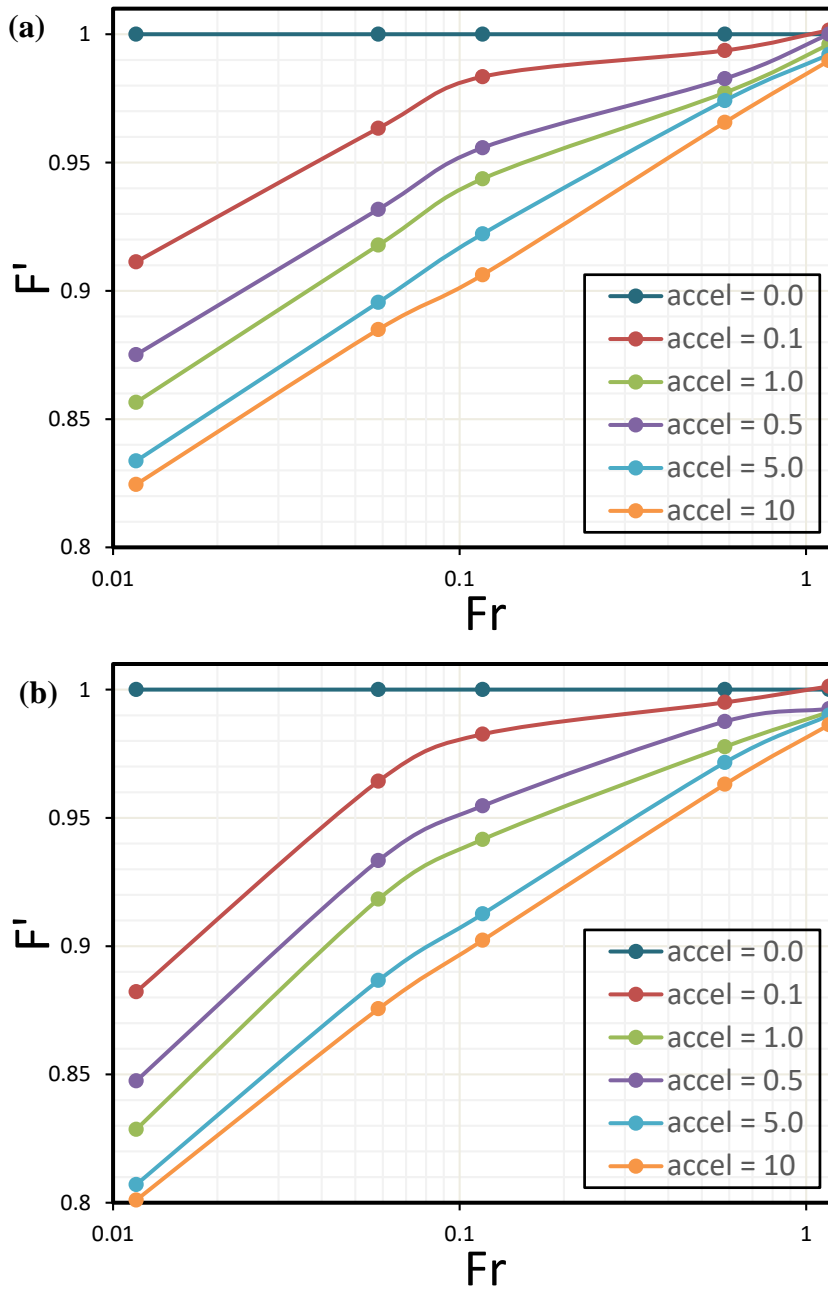


**Figure 4-2:** Non-dimensional drag force plotted against Froude number different accelerations (a) Particle Density 2500 kg/m<sup>3</sup> (b) Particle Density 5000 kg/m<sup>3</sup>

### 4.1.2 Effect of particle stiffness on virtual mass force

Changing particle stiffness from 800N/m to 8000N/m reduces drag by 2.8% and 3.2% for  $0.1m/s^2$  acceleration and  $10m/s^2$  acceleration respectively as shown in Error! Reference source not found.

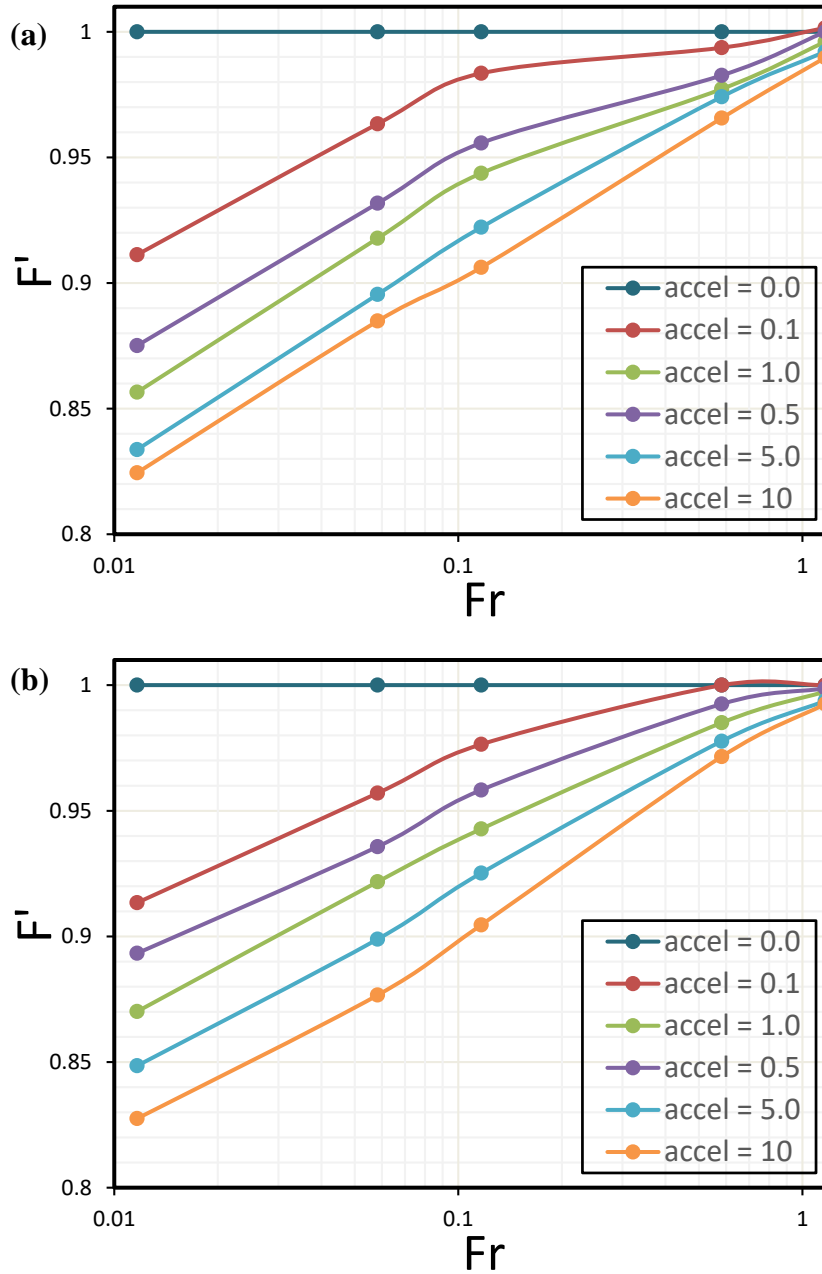


**Figure 4-3:** Non-dimensional drag force plotted against Froude number for different accelerations (a) Particles stiffness 800N/m (b) Particles stiffness 8000N/m

### 4.1.3 Effect of particle coefficient of restitution on virtual mass force

Changing particle coefficient of restitution from 0.7 to 0.2 reduces drag by 0.7% for and 3.2% for  $0.1m/s^2$  acceleration and  $10m/s^2$  acceleration respectively. Also note the saturation of drag force at high acceleration for 0.2 coefficient of restitution.

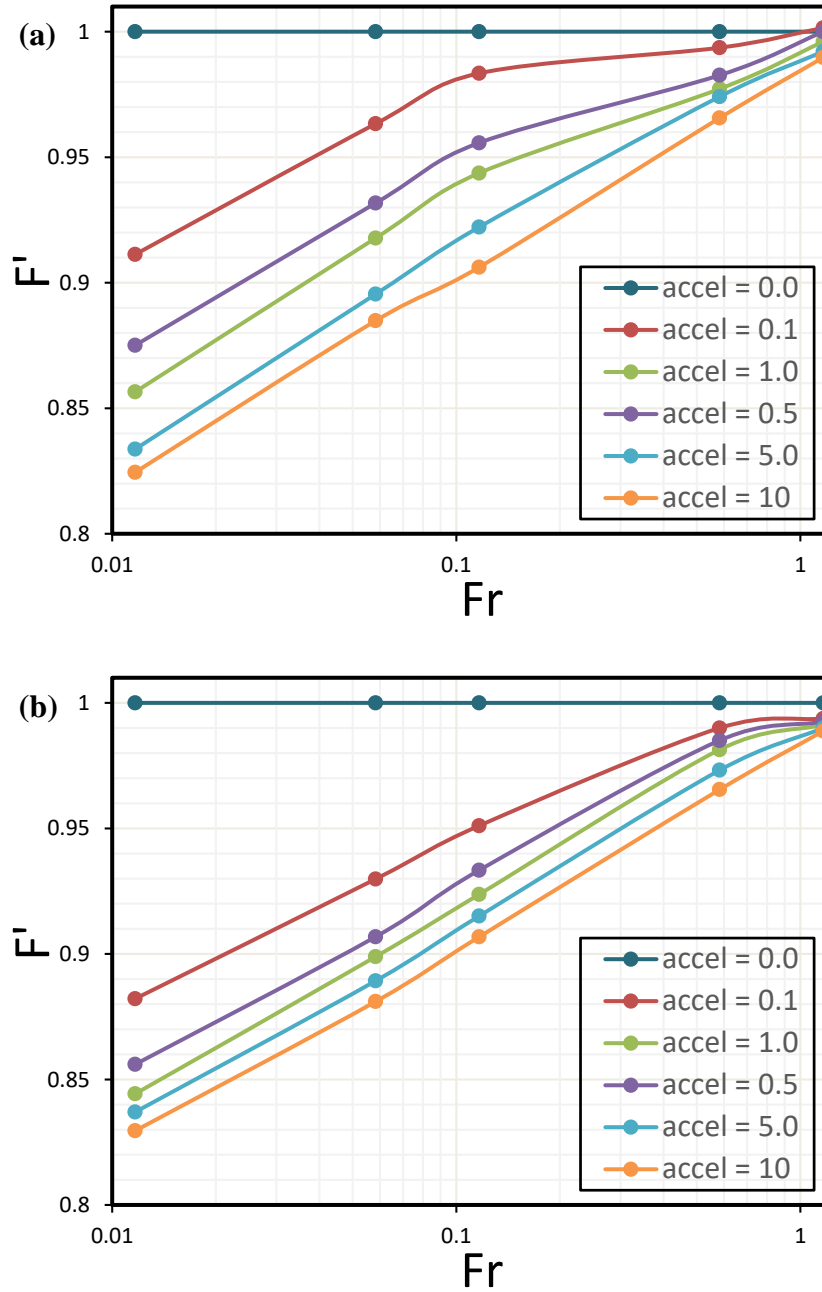


**Figure 4-4:** Non-dimensional drag force plotted against Froude number for different accelerations (a) Coefficient of restitution 0.7 (c) Coefficient of restitution 0.2

#### 4.1.4 Effect of particle friction coefficient on virtual mass force

Changing particle friction has the most significant effect on the unsteady granular drag. For 0.01 Froude number changing particle coefficient of friction from 0.1 to 0.5 reduces drag by 3.0% and 4.4% for  $0.1m/s^2$  acceleration and  $10m/s^2$  acceleration respectively. Among the material parameters studies increasing coulomb friction to 0.5 records maximum drag force reduction of 17.6% compared to steady motion. This is behavior can be related to the fact that for  $Fr < 1$  drag force is mainly due to frictional effect.

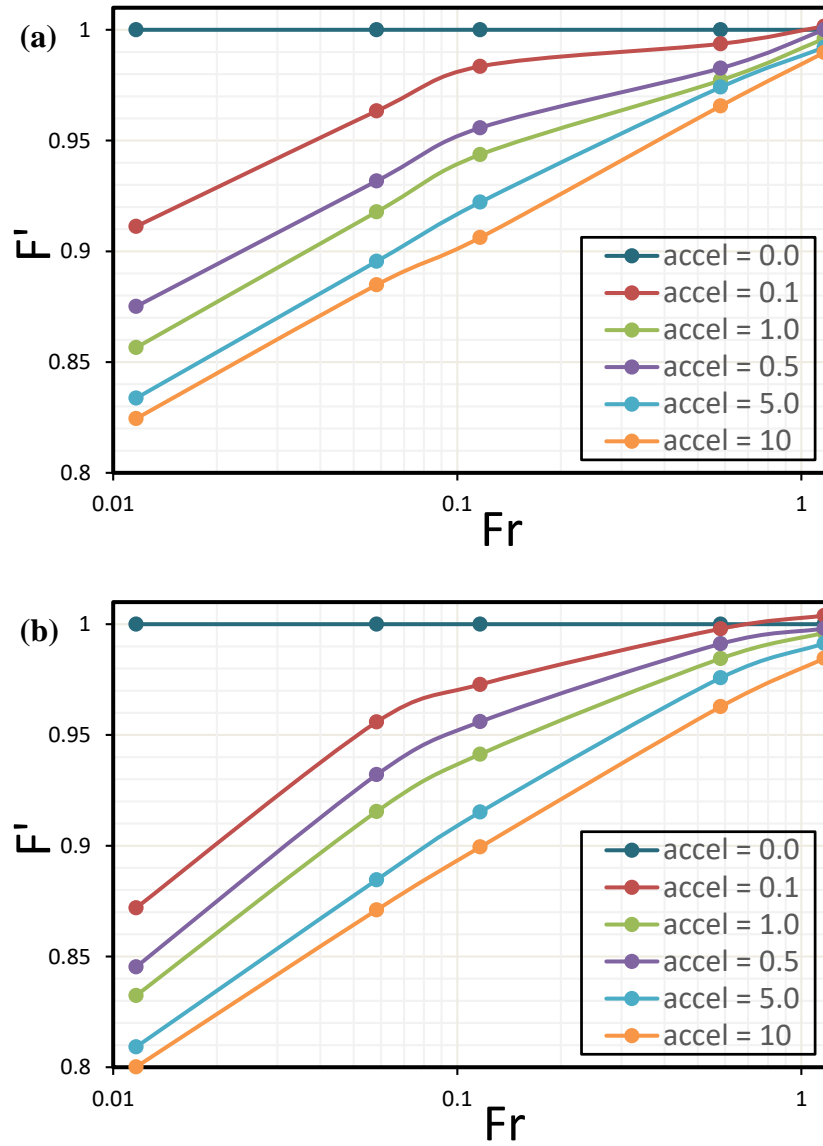


**Figure 4-5:** Non-dimensional drag force plotted against Froude number for different accelerations (a) Coefficient of Friction 0.1 (b) Coefficient of Friction 0.5

In granular media, force is transferred via force chains(I. Albert et al., 2001; Cates, Wittmer, Bouchaud, & Claudin, 1998) and the particle mass moving with intruder at any instant is determined by the strength and stability of force chains. Force chains are very susceptible to external disturbances and can be easily broken from external disturbances such as vibrations(Cates et al., 1998; Claudin & Bouchaud, 1998; Claudin, Bouchaud, Cates, & Wittmer, 1998; Liu & Nagel, 1998). Thus, it can be argued that the unsteady motion of intruder leads to the formation of weaker and more unstable force chains than its steady counterpart. These weaker force chains result in less drag for unsteady cases discussed earlier. This can be verified by identifying the particles being accelerated with intruder. Figure 4-6 shows particles' velocity as a fraction of intruders velocity. It can be observed that maximum particles are being accelerated with the intruder when intruder is moving with uniform velocity while the number of accelerated particles decrease when intruder is moving with non-uniform velocity.

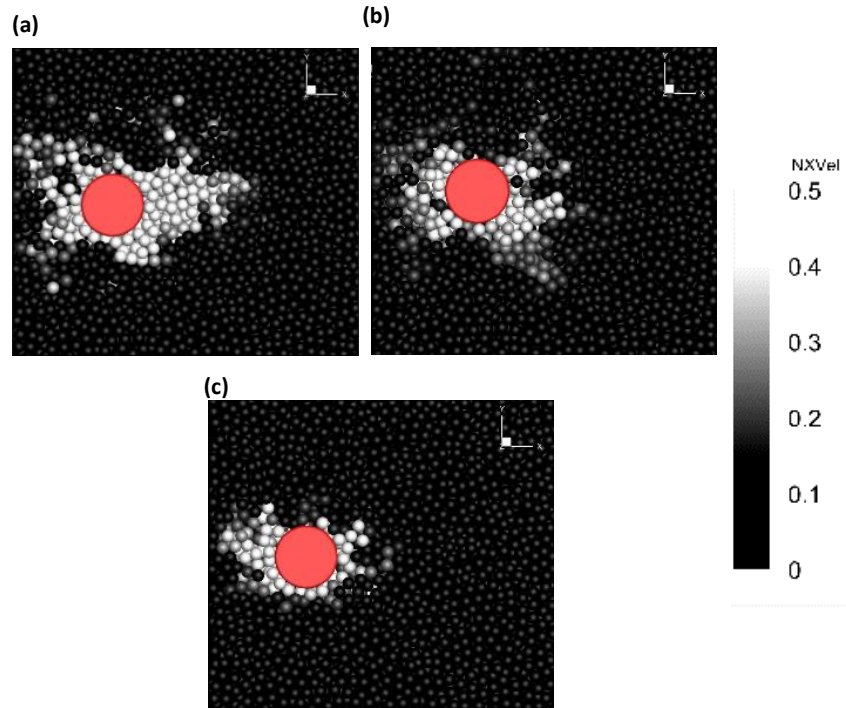


**Figure 4-6** Particles accelerated with intruder ( $NXVel = V_{intruder}/V_{particles}$ ) for Froude 0.01  
(a) acceleration 0 m/s<sup>2</sup> (b) acceleration 0.1 m/s<sup>2</sup> (d) acceleration 10 m/s<sup>2</sup>

This behavior of drag force can be expressed in virtual mass force like manner as shown in Eqn. 4.1

$$F'_{total} = F'_{steady} - F'_{unsteady} \quad (4.1)$$

From previous data we determine the  $F'_{unsteady}$  to be a power function of form shown in Eqn. 4.2.

$$F'_{unsteady} = ax^b + c \quad (4.2)$$

Where  $a, b, c$  are fit coefficients given in Eqn. 4.2. These coefficients depend on acceleration as well as material properties of the particles. Figure 4-7 shows Eq. 4.2 fitted to baseline case with these coefficients.

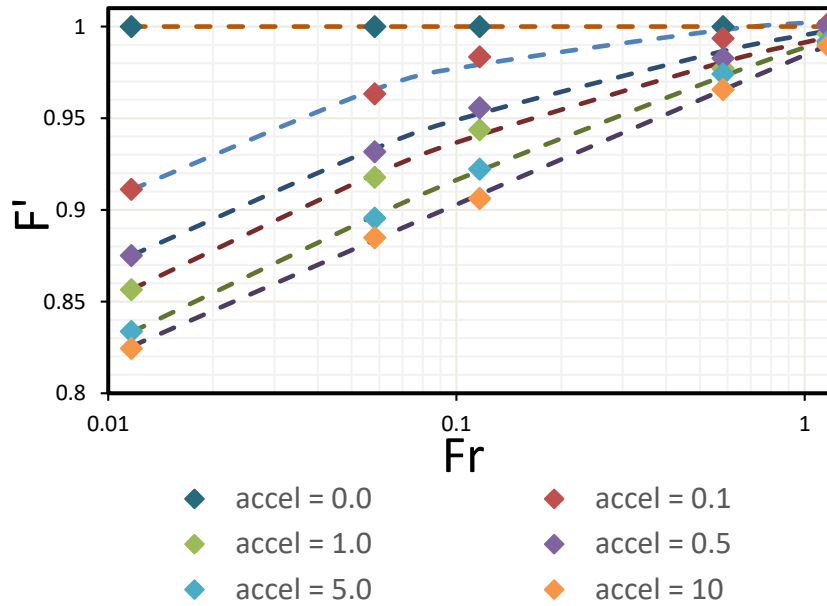


**Figure 4-7** Non-dimensional drag force plotted against Froude number for different accelerations. Discrete points represent simulation results and dotted line represent Eqn. 4.2 with appropriate fitting parameters

**Table 4-1:** Fit coefficients

Acceleration ( $m/s^2$ )	Fit Coefficients		
	$a$	$b$	$c$
0.1	-0.0134	-0.4612	1.0154
0.5	-0.0657	-0.2337	1.0611
1.0	-0.0948	-0.1986	1.0861
5.0	-0.3138	-0.0903	1.3024
10	-4.5558	-0.0077	5.5402

## CHAPTER 5: CONCLUSION

DEM simulations to study unsteady granular drag force on an intruder moving with non-uniform velocity have been performed. Comparison with steady drag shows that in quasi-static regime ( $Fr < 1$ ) an accelerating intruder experiences a reduced drag than its non-accelerating counterpart and increasing the acceleration of the intruder further decreases the drag on intruder. A 17.6% reduction in drag compared to steady motion is observed for acceleration of  $10 \text{ m/s}^2$ . This behavior is in contrast with the fluids where a body accelerating relative to fluid medium experiences more drag due to the acceleration of surrounding fluid. This unique behavior is found to be caused due to less particle mass being accelerated with intruder as a consequence of weaker force chain formation due to unsteady nature of intruder motion. This behavior is found to be independent of particle material properties such as stiffness coefficient, density, coefficient of friction and coefficient of restitution. Changing particle material properties, however, changes the amount of drag reduction. The unsteady drag, like fluids, can be split into steady component and a negative virtual mass component as given in Eq. 4.1.



## **CHAPTER 6: FUTURE RECOMMENDATIONS**

The future recommendations for extension of this study are the following:

- Increase number of intruders and examine drag force on each intruder.
- Consider staggered arrangement of intruders for higher number of intruders.
- Vary immersion depth and study the corresponding effect on drag force.
- Fluidize the granular bed and inspect the effect on drag reduction.
- Parallelize the DEM code.

## REFERENCES

- Aguilar, J., & Goldman, D. I. (2016). Robophysical study of jumping dynamics on granular media. *Nature Physics*, 12(3), 278.
- Albert, I., Tegzes, P., Albert, R., Sample, J. G., Barabási, A.-L., Vicsek, T., ... Schiffer, P. (2001). Stick-slip fluctuations in granular drag. *Physical Review E*, 64(3), 31307.
- Albert, R., Pfeifer, M. A., Barabási, A.-L., & Schiffer, P. (1999). Slow drag in a granular medium. *Physical Review Letters*, 82(1), 205.
- Antony, S. J., Hoyle, W., & Ding, Y. (2004). *Granular materials: fundamentals and applications*. Royal Society of Chemistry.
- Athani, S., & Rognon, P. (2019). *Inertial drag in granular media*. Retrieved from <http://arxiv.org/abs/1907.05613>
- Bishop, S. R., Momiji, H., Carretero-González, R., & Warren, A. (2002). Modelling desert dune fields based on discrete dynamics. *Discrete Dynamics in Nature and Society*, 7(1), 7–17.
- Brennen, C. E. (1982). *A Review of Added Mass and Fluid Inertial Forces*.
- Cates, M. E., Wittmer, J. P., Bouchaud, J.-P., & Claudin, P. (1998). Jamming, force chains, and fragile matter. *Physical Review Letters*, 81(9), 1841.
- Chehata, D., Zenit, R., & Wassgren, C. R. (2003). Dense granular flow around an immersed cylinder. *Physics of Fluids*, 15(6), 1622–1631. <https://doi.org/10.1063/1.1571826>
- Claudin, P., & Bouchaud, J.-P. (1998). Stick-slip transition in the Scalar Arching Model. *Granular Matter*, 1(2), 71–74.
- Claudin, P., Bouchaud, J.-P., Cates, M. E., & Wittmer, J. P. (1998). Models of stress fluctuations in granular media. *Physical Review E*, 57(4), 4441.
- Cundall, P. A., & Strack, O. D. L. (1979). A discrete numerical model for granular assemblies. *Geotechnique*, 29(1), 47–65.
- Darve, F., & Laouafa, F. (2000). Instabilities in granular materials and application to landslides. *Mechanics of Cohesive-Frictional Materials: An International Journal on Experiments, Modelling and Computation of Materials and Structures*, 5(8), 627–652.
- Fan, F., Parteli, E. J. R., & Pöschel, T. (2017). Origin of granular capillarity revealed by particle-based simulations. *Physical Review Letters*, 118(21), 218001.
- Geng, J., & Behringer, R. P. (2005). Slow drag in two-dimensional granular media. *Physical Review E*, 71(1), 11302.
- Goldfarb, D. J., Glasser, B. J., & Shinbrot, T. (2002). Shear instabilities in granular flows. *Nature*, 415(6869), 302–305. <https://doi.org/10.1038/415302a>
- Hilton, J. E., & Tordesillas, A. (2013). Drag force on a spherical intruder in a granular bed at low

- Froude number. *Physical Review E*, 88(6), 62203.
- Jaeger, H. M., Nagel, S. R., & Behringer, R. P. (1996). Granular solids, liquids, and gases. *Reviews of Modern Physics*, 68(4), 1259.
- Ji, S., & Shen, H. H. (2006). Effect of contact force models on granular flow dynamics. *Journal of Engineering Mechanics*, 132(11), 1252–1259.
- Katsuragi, H., & Durian, D. J. (2007). Unified force law for granular impact cratering. *Nature Physics*, 3(6), 420–423. <https://doi.org/10.1038/nphys583>
- Katsuragi, H., & Durian, D. J. (2014, January 29). Erratum: Drag force scaling for penetration into granular media (Physical Review E (2013) 87 (052208)). *Physical Review E - Statistical, Nonlinear, and Soft Matter Physics*, Vol. 89. <https://doi.org/10.1103/PhysRevE.89.019902>
- Kumar, S., Dhiman, M., & Reddy, K. A. (2019). Magnus effect in granular media. *Physical Review E*, 99(1), 12902.
- Kumar, S., Reddy, K. A., Takada, S., & Hayakawa, H. (2017). Scaling law of the drag force in dense granular media. *ArXiv Preprint ArXiv:1712.09057*.
- Liu, A. J., & Nagel, S. R. (1998, November 5). Jamming is not just cool any more. *Nature*, Vol. 396, pp. 21–22. <https://doi.org/10.1038/23819>
- Lohse, D., Rauhe, R., Bergmann, R., & Van Der Meer, D. (2004). Creating a dry variety of quicksand. *Nature*, 432(7018), 689–690.
- Malone, K. F., & Xu, B. H. (2008). Determination of contact parameters for discrete element method simulations of granular systems. *Particuology*, 6(6), 521–528.
- Mishra, B. K., & Murty, C. V. R. (2001). On the determination of contact parameters for realistic DEM simulations of ball mills. *Powder Technology*, 115(3), 290–297.
- Nelson, E. L., Katsuragi, H., Mayor, P., & Durian, D. J. (2008). Projectile interactions in granular impact cratering. *Physical Review Letters*, 101(6), 68001.
- Okorie, O. (2017). Micromechanical Analysis of Compaction and Drilling of Granular Media-A Review. *International Journal of Chemical Engineering and Processing*, 3(2), 1–6.
- Prado, G., Amarouchene, Y., & Kellay, H. (2011). Experimental evidence of a rayleigh-plateau instability in free falling granular jets. *Physical Review Letters*, 106(19), 198001.
- Reddy, A. V. K., Kumar, S., Reddy, K. A., & Talbot, J. (2018). Granular silo flow of inelastic dumbbells: Clogging and its reduction. *Physical Review E*, 98(2), 22904.
- Reynolds, O. (1885). LVII. On the dilatancy of media composed of rigid particles in contact. With experimental illustrations. *The London, Edinburgh, and Dublin Philosophical Magazine and Journal of Science*, 20(127), 469–481.
- Rhodes, M. J. (1990). *Principles of powder technology*.

- Rojek, J. (2018). Contact Modeling in the Discrete Element Method. In *Contact Modeling for Solids and Particles* (pp. 177–228). Springer.
- Seguin, A., Bertho, Y., & Gondret, P. (2008). Influence of confinement on granular penetration by impact. *Physical Review E*, 78(1), 10301.
- Soller, R., & Koehler, S. A. (2006). Drag and lift on rotating vanes in granular beds. *Physical Review E*, 74(2), 21305.
- Takada, S., & Hayakawa, H. (2017). Drag law of two-dimensional granular fluids. *Journal of Engineering Mechanics*, 143(1), C4016004.
- Tijsskens, E., Ramon, H., & De Baerdemaeker, J. (2003). Discrete element modelling for process simulation in agriculture. *Journal of Sound and Vibration*, 266(3), 493–514.
- Tsimring, L. S., & Volfson, D. (2005). Modeling of impact cratering in granular media. *Powders and Grains*, 2, 1215–1223.
- Umbanhowar, P., & Goldman, D. I. (2010). Granular impact and the critical packing state. *Physical Review E*, 82(1), 10301.
- Vinningland, J. L., Johnsen, Ø., Flekkøy, E. G., Toussaint, R., & Måløy, K. J. (2007). Granular rayleigh-taylor instability: Experiments and simulations. *Physical Review Letters*, 99(4), 48001.

# Study of granular drag force for intruder moving with non-uniform velocities using Discrete Element Method

*by* Husnain Murtaza

---

**Submission date:** 07-Sep-2020 05:09PM (UTC+0500)

**Submission ID:** 1381339538

**File name:** 27216\_Husnain\_Murtaza\_Study\_of\_granular\_drag\_force\_for\_intruder\_moving\_with\_non-uniform\_velocities\_using\_Discrete\_Element\_Method\_560\_1669080387.pdf (2.31M)

**Word count:** 5888

**Character count:** 38081

# Study of granular drag force for intruder moving with non-uniform velocities using Discrete Element Method

## ORIGINALITY REPORT

6%

SIMILARITY INDEX

2%

INTERNET SOURCES

5%

PUBLICATIONS

0%

STUDENT PAPERS

## PRIMARY SOURCES

- |   |   |    |
|---|---|----|
| 1 | Ali Abbas Zaidi. "Granular drag force during immersion in dry quicksand", Powder Technology, 2020<br>Publication  | 2% |
| 2 | <a href="http://era.library.ualberta.ca">era.library.ualberta.ca</a><br>Internet Source   | 1% |
| 3 | <a href="http://linknovate.com">linknovate.com</a><br>Internet Source   | 1% |
| 4 | Ali Abbas Zaidi, Christoph Müller. "Vertical drag force acting on intruders of different shapes in granular media", EPJ Web of Conferences, 2017<br>Publication | 1% |
| 5 | J. E. Hilton, A. Tordesillas. "Drag force on a spherical intruder in a granular bed at low Froude number", Physical Review E, 2013<br>Publication               | 1% |
| 6 | Abd El-Rahman, M.K.. "Industrial tumbling mill power prediction using the discrete element  | 1% |

# method", Minerals Engineering, 200110

Publication

---

---

Exclude quotes      Off

Exclude matches      < 1%

Exclude bibliography      On